ACS OMEGA

http://pubs.acs.org/journal/acsodf

Article

Unsaturated Polyester Resin Filled with Cementitious Materials: A Comprehensive Study of Filler Loading Impact on Mechanical Properties, Microstructure, and Water Absorption

Salah M. S. Al-Mufti,* Asma Almontasser, and Syed J. A. Rizvi*

Cite This: *ACS Omega* 2023, 8, 20389−20403

Read Online

ACCESS | Metrics & More | Article Recommendations

ABSTRACT: In recent years, cheaply available cementitious materials (CMs) are increasingly finding useful applications in construction engineering. This manuscript focused on the development and fabrication of unsaturated polyester resin (UPR)/cementitious material composites to be potentially useful in a variety of construction applications. For this purpose, five types of powders from widely available fillers, i.e., black cement (BC), white cement (WC), plaster of Paris (POP), sand (S), and pit sand (PS), were used. Cement polymer composite (CPC) specimens were prepared by a conventional casting process with various filler contents of 10, 20, 30, and 40 wt %. Neat UPR and CPCs were investigated mechanically by testing their tensile, flexural, compressive, and impact properties. Electron microscopy analysis was used to analyze the relation between the microstructure and mechanical properties of CPCs. The assessment of water absorption was conducted. The highest tensile, flexural, compressive upper yield, and impact strength values were recorded for POP/UPR-10, WC/UPR-10, WC/UPR-40, and POP/UPR-20, respectively. The highest percentages of water absorption were found to be 6.202 and 5.07% for UPR/BC-10 and UPR/BC-20, while the lowest percentages were found to be 1.76 and 1.84% for UPR/S-10 and UPR/S-20, respectively. Based on the finding of this study, the properties of CPCs were found to depend on not only the filler content but also the distribution, particle size, and combination between the filler and the polymer.

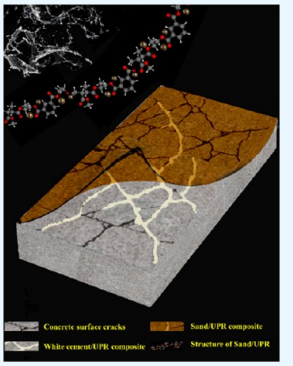

1. INTRODUCTION

The use of composite materials has been significantly increasing in several industrial fields worldwide. It is well known that a composite material is a material system that is produced from a combination of two or more phases on a macroscopic scale; their physical and chemical properties and mechanical performance are designed to be superior to those of the constituent materials acting independently. One of the phases, which is discontinuous, usually stiffer, and stronger, is called the reinforcement, whereas the less stiff and weaker phase is continuous and is called the matrix. In most of the industrial applications, the properties of polymers are modified using fillers. As an outstanding advancement in the polymer industry, particulate fillers have been used as reinforcements in the polymer matrix. In recent years, there has been considerable interest in using particulate fillers, not only from an economic viewpoint but also as modifiers, especially the physical properties of the polymer.[1] Research is underway worldwide to develop newer cement composites (CCs) with varied combinations of fillers such as graphene, graphene oxide, reduced graphene oxide, carbon nanotubes, carbon fiber, and others so as to make them usable under different operational conditions.[2−6] Over the past few decades, there has been a growing interest in materials science and metallurgy in the synthesis and characterization of polymer−matrix, ceramic−matrix, and metal matrix composites for a variety of applications.[7−11] Out of these, polymer−matrix composites are very important as they are most widely used because of their unique properties like ease of fabrication, lightness, low cost, water resistance, corrosion resistance, and a variety of other properties.[12] Two types of polymers are used in construction: thermoset and thermoplastic polymers. Thermosets such as epoxy,[13] unsaturated polyester (UPR), vinyl ester (VE),[14,15] etc. are being increasingly used in several applications, e.g., solid resin and terrazzo flooring, anchor fixings, adhesives, FRP bridge sections, cladding panels, sinks, surfaces, and coatings.[16] Likewise, thermoplastic polymers, for instance, expanded polystyrene (EPS), polypropylene (PP), poly(vinyl chloride) (PVC), polyurethane (PU), etc., are used in concrete molds, insulation, packaging, sound insulation, water pipes, waste pipes, sealants, and concrete jointing.

The primary binder of ordinary Portland concrete (OPC) is cement, which causes decreased tensile strength and significant dry shrinkage deformation when the material cures. Addition-

Received: January 17, 2023
Accepted: May 19, 2023
Published: May 30, 2023

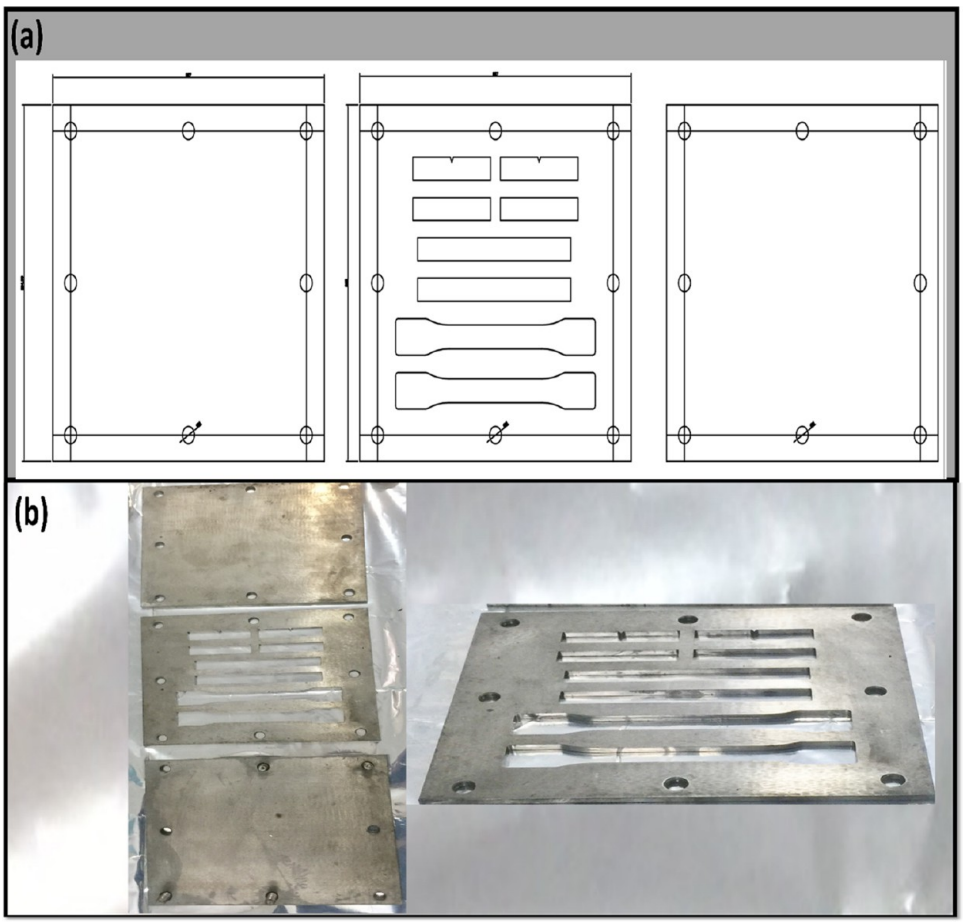

Figure 1. Steel mold used to fabricate the cement polymer composites: (a) design and (b) manufactured.

ally, workability and applicability needs of OPC may be constrained by the low temperature and long curing time. The chemical corrosion resistance of OPC is also subpar. OPC frequently falls short of certain critical environments and high-quality engineering criteria. In order to improve the durability and mechanical properties of concrete, polymer concrete (PC) can be employed. PC is usually prepared by the incorporation of polymers such as epoxy, UPR, or VE compounds as coating materials or can be used as additive materials.[17] These three types of polymers are frequently employed, and based on how they are utilized, they can make several types of concretes, including PC, polymer-impregnated concrete (PIC), and polymer−cement concrete (PCC).[18] PC, in general, has a much-accelerated strength development rate than ordinary concretes and thus is used to produce high-strength concretes possessing anticorrosion and chemical-resistant properties. PC begins its crosslinking network reaction to connect with the surrounding materials by utilizing a thermosetting resin, which acts as a curing agent. PC is prepared in two parts, using the sand and gravel as an aggregate and using the synthetic resin (organic polymer) or monomer as a binder for the aggregates. It is widely used in bonding materials, anticorrosion materials, base plate materials, prefabricated components, and waterproof materials because of its advantages in insulation, fast curing at low temperature, strength, chemical corrosion resistance, water tightness, wear resistance, and higher elastic modulus than OPC and asphalt concrete.[19]

Unsaturated polyester resin concrete (UPRC) is a synthetic compound concrete. UPRC is made up of UPR with fillers, fine aggregates, and a certain proportion of coarse aggregates. As compared with OPC, UPR is used in UPC instead of cement to act as a binder in the concrete mixture to produce sustainable concrete.[20,21] UPRC contains roughly 90% fillers and 10% UPR and additives.[22] The construction performance and mechanical properties of UPRC are largely related to the curing process of unsaturated resin, in which the curing process will directly affect the mechanical properties of UPRC. However, UPRC often shows high viscosity while stirring for the presence of resins, and high-speed mechanical mixing with forced agitation must be used during the mixing as compared to OPC. According to their applications, composite materials are prepared via various techniques, such as conventional casting, sheet molding compound, pultrusion, bulk molding compound, resin transfer molding, etc.[23] UPR is widely used in composite materials due to its low cost, easy processing, heat resistance, humidity resistance, and good mechanical and insulating properties.[24,25]

Some researchers have prepared inorganic powders/thermoset (UPR, EP, and VE) composites and investigated their properties. Heriyanto et al.[26] synthesized waste powder filler/epoxy composites and reported that adding an amino silane coupling agent in the composite can improve the strength and adhesion between the inorganic fillers and the organic epoxy resin. Chowaniec et al.[27] pointed that quartz powders can be loaded up to 29 wt % in epoxy coatings without losing their adhesive properties. Erkliğ et al.[28] prepared sewage sludge ash (SSA), fly ash (FA), and silicon carbide (SiC)/UPR composites and investigated the mechanical properties of composites. They found that the highest values of tensile and flexural strength were

https://doi.org/10.1021/acsomega.3c00353
ACS Omega 2023, 8, 20389−20403

52 and 109.9 MPa for UPR/SiC and UPR/FA (95/5) wt %, respectively. Tabatabai et al.[29] used flue-gas desulfurization (FGD) gypsum to enhance the mechanical properties of UPR. The results of the UPR showed an improvement in mechanical properties by the addition of a (FGD) gypsum filler. Using the hand lay-up technique, Ahmad et al.[30] developed silica nanoparticles/glass fibers/UPR composites and reported that with addition of 4 wt % of both fillers the tensile strength of composites reached up to 78 MPa. de Souza et al.[31] studied the mechanical properties of UPR filled with BC and pointed out that the tensile, flexural, and impact strengths decreased with increasing filler content. Singer et al.[32] investigated the time-dependent changes of the mechanical properties of the VE/EP/filler (quartz/cement) composite and found that the strength of VE/filler composites increased with time and curing temperature, while the strength of EP/filler composites increased at higher postcuring temperatures. Shettar et al.[33] used BC to improve the properties of glass fiber/UPR composites for coating of fishing boats and observed that the addition of BC leads to enhancing the mechanical properties.

Studies related to UPR/cementitious material composites are hardly available in the literature, but UPRC and ceramic composites have been extensively studied. This manuscript aims to develop and fabricate unsaturated polyester resin (UPR)/cementitious material (black cement (BC), white cement (WC), plaster of Paris (POP), sand (S), and pit sand (PS)) composites and assess their mechanical properties for possible applications in construction. The study seeks to deepen the understanding of the behavior of UPR/cementitious composites and their potential use in areas such as infrastructure repair, construction coatings, and structural reinforcement. By exploring the feasibility of UPR/cementitious composites as substitutes for traditional construction materials, the paper aims to provide a foundation for future research in this field.

2. MATERIALS AND METHODS

2.1. Materials. Unsaturated polyester resin (UPR), cobalt naphthenate, and methyl ethyl ketone peroxide (MEKP) were obtained from Shri Shyam Polymers, New Delhi, India. Shree cement OPC 43 grade (BC), J.K. white cement (WC), plaster of Paris (POP), sand (S), pit sand (PS), mold release agent, and polyester nylon blended fabric (PNBF) were purchased from local markets of Aligarh-India. All of the materials were used as such without purifying any further. It is worth noting that sand and pit sand were sifted manually through a No. 50 (300 μm) sieve to remove unwanted large particles.

2.2. Stainless Steel Mold. According to ASTM standards, a stainless steel mold has been manufactured to produce the specimens of the composite in the National Small Industries Corporation Ltd., Aligarh, India. To facilitate ease of fabrication, easy removal of specimen, and cleaning, a three-plate mold was fabricated from stainless steel (Grade EN 31). The mold contained of an upper plate, a lower plate, and a mold cavity (see Figure 1a,b).

2.3. Composite Manufacturing Process. Cement polymer composites were prepared via conventional casting in a stainless steel mold. Figure 2 illustrates the preparation process. CPCs were synthesized by two steps: mixing process and casting process.

2.3.1. Mixing Process. First, neat UPR was degassed in a vacuum oven (30 Hg) for 10 min at RT to remove air bubbles. Cobalt naphthalene as the accelerator (0.3 wt % UPR weight as suggested by the supplier) was added to UPR and mixed for a few minutes. A certain amount of cement was added to UPR and mixed properly. The concentration of cement added in the resin was varied from 10 to 40 wt % by weight of UPR (see Table 1).

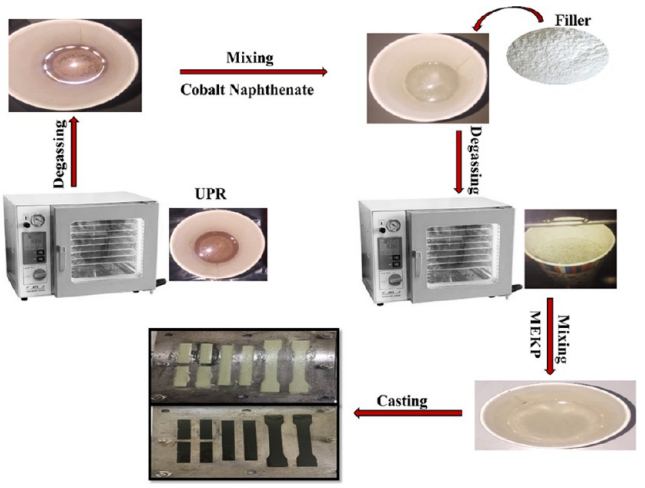

Figure 2. Schematic diagram of the synthetic procedure for the preparation of UPR/cement composites.

Table 1. Composition and Nomenclature of Cement Polymer Composites (CPCs)

composites	composition (wt %)
UPR/WC-10, UPR/BC-10, UPR/POP-10, UPR/S-10, UPR/PS-10	90/10 (UPR/filler)
UPR/WC-20, UPR/BC-20, UPR/POP-20, UPR/S-20, UPR/PS-20	80/20 (UPR/filler)
UPR/WC-30, UPR/BC-30, UPR/POP-30, UPR/S-30, UPR/PS-30	70/30 (UPR/filler)
UPR/WC-40, UPR/BC-40, UPR/POP-40, UPR/S-40, UPR/PS-40	60/40 (UPR/filler)

To remove bubbles generated during the mixing process, the mixture was degassed in a vacuum oven until the air bubbles were removed completely, as shown in Figure 3. MEKP (hardener), 1.5 wt % UPR weight as suggested by the manufacturer, was added to the mixture and mixed for 2 min.

2.3.2. Casting Process. For easy separation of the prepared specimens from a mold, silicone spray (releasing agent) was sprayed on the mold. In addition, a Polyester Nylon Blended Fabric was used to gain good surface finish (see Figure 3). The mixture was poured into a stainless steel mold, and then, the mixture surface was carefully leveled. Within 5−10 min, the mixture achieved the gel state and cured within 20−30 min. However, the composite was allowed to stand for 24 h at RT. Then, the specimens were demolded for further characterization. For compressive testing samples, the casting process was done in a glass tube according to ASTM D695. This manufacturing method is simple, potentially cost-effective, and scalable for mass production. The prepared specimens of CPCs are shown in Figure 4.

2.4. Characterization. The tests of tensile, flexural, and compressive properties of the CPC specimens were carried out using a universal testing machine (UTM). Tensile, flexural, and compressive properties of the CPC specimens were performed at constant strain rates of 20, 5, and 5 mm/min, respectively. The tests of tensile, flexural, and compressive properties were conducted according to the ASTM D638,[34] ASTM D790,[35]

https://doi.org/10.1021/acsomega.3c00353
ACS Omega 2023, 8, 20389−20403

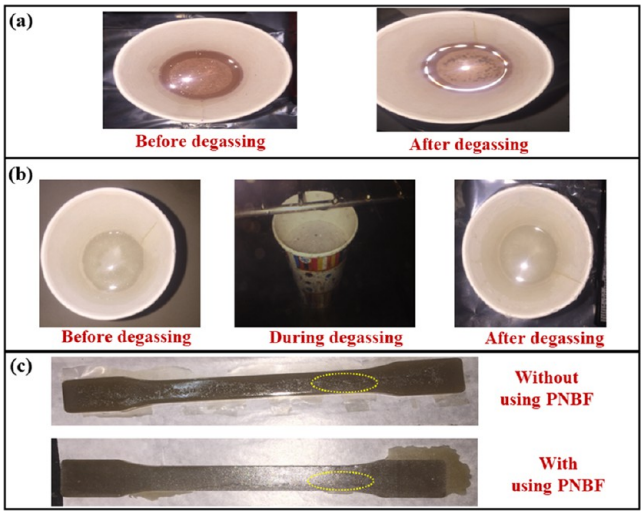

Figure 3. Schematic illustrating: (a) Degassing process of UPR, (b) Degassing process of composite, and (c) The influence of using PNBF on prepared composite specimens. The yellow dotted circle in the image of (c) highlights the smooth surface without the appearance of any bubbles after using PNBF.

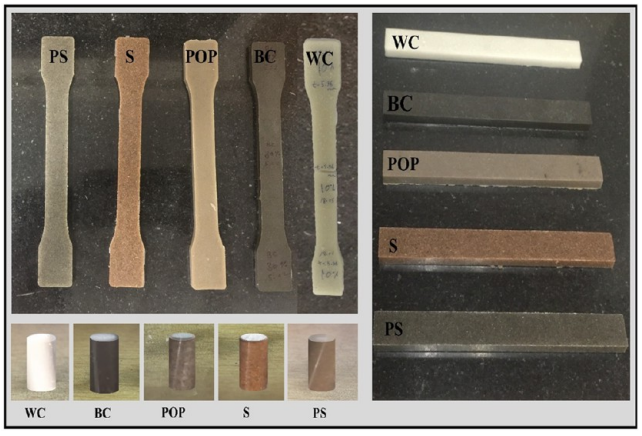

Figure 4. Top-view photograph of cement polymer composite standard test specimens.

and ASTM D695[36] standards, respectively. The Izod/Charpy impact tester was used to test the impact strength of CPC samples. The impact test was applied to the CPC specimens according to ASTM D256.[37] The water absorption test of CPCs was performed as referred to in the ASTM D570-98 standard. At least three samples were repeated for each test.

3. RESULTS AND DISCUSSION

Cement polymer composites have been developed with various quantities of UPR, WC, POP, BC, S, and PS. The details of the influence of filler contents with the UPR matrix on mechanical properties in terms of tensile, flexural, compressive, impact, and water absorption properties have been tested and discussed in the following section.

3.1. Mechanical Properties of the Cement Polymer Composite. *3.1.1. Tensile Properties.* The tensile strength of the cement polymer specimens was performed at a constant strain rate of 20 mm/min. Tensile strength properties of the control (neat UPR) with different percentages of CPCs are shown in Figure 5a and Table 2. It can be seen in Figure 5a that there is a decrease in the tensile strength of CPCs as compared to the control. The filler contents in the UPR/WC, UPR/POP, UPR/S, and UPR/PS composites resulted in a systematic decrease in their tensile strength from 10 to 40%, whereas the UPR/BC composite exhibited an unsystematic decrease (refer to Table 2). The polymer composites of S and PS exhibited the lowest values of the tensile strength (16.813, 16.835 MPa) at 40 wt % fillers. UPR/BC and UPR/POP composites showed better tensile strength in compression with UPR/WC, UPR/S, and UPR/PS composites (see Figure 5a). The tensile strength of the UPR/BC composite varied between 32.337 and 36.564 MPa. The tensile fracture surface of specimens is shown in Figure 8. The unsystematic variation in tensile strength values of the UPR/BC composite could be due to distribution of fillers in a disorderly manner and unsystematically in the matrix. Among the CPC specimens, the highest tensile strength value (37.413 MPa) was found with UPR/POP at a low weight ratio (10 wt %), which could be due to the strong bonding between UPR and POP as a result of the very small particle size and good distribution of filler particles.[38,39] The UPR resin is a type of thermosetting polymer that can form a strong chemical bond with many types of fillers, including POP powder. The chemical bonds between the resin and filler molecules can create a high-strength interfacial region, which can resist deformation and failure under tensile loads. Additionally, the UPR resin can penetrate into the porous structure of the POP powder, creating a mechanical interlocking effect that further enhances the bond strength. The UPR resin can act as a matrix that binds the POP powder particles together, creating a cohesive structure that resists deformation and fracture.

Figure 5b and Table 3 illustrate Young's modulus values of neat UPR and CPCs with different ratios of fillers. Young's modulus of the specimens of UPR/S and UPR/PS composites exhibited lower values for all of the filler concentrations than the value of neat UPR (0.628 GPa), while Young's modulus of the UPR/POP composite varied over the range of 0.495−0.723 GPa. The result showed that the experimentally determined Young's moduli of UPR/WC and UPR/BC composites for all filler concentrations (from 10 to 40 wt %) were higher than those of neat UPR and UPR/POP composites. Young's moduli of UPR/WC composites increased systematically as the filler ratio was increased, while the increases in UPR/BC values were somewhat unsystematic (see Figure 5b). At 40 wt % BC, CPCs of UPR/BC showed the highest value (0.878 GPa) of Young's modulus as compared to the other specimens (see Table 3). In the case of UPR/WC composites, the increase in the filler ratio leads to an increase in the volume fraction of the high-stiffness ceramic filler (WC), which contributes significantly to the overall stiffness of the composite. As the proportion of the filler increases, the filler becomes more uniformly distributed throughout the matrix, leading to a more homogeneous microstructure and a more effective load transfer between the filler and the matrix. These factors contribute to the systematic increase in Young's modulus observed in UPR/WC composites as the filler ratio is increased. However, the behavior of UPR/BC composites is somewhat more complex. Although an increase in filler content can lead to an increase in stiffness, this effect can be offset by other factors such as the agglomeration of filler particles or the formation of voids in the matrix. Moreover, the surface chemistry and morphology of the filler can play a significant role in determining the strength of the filler−matrix interface, which affects the overall stiffness of the composite. These factors can lead to a less systematic increase in Young's modulus observed in UPR/BC composites as the filler ratio is increased. Therefore, it

https://doi.org/10.1021/acsomega.3c00353
ACS Omega 2023, 8, 20389−20403

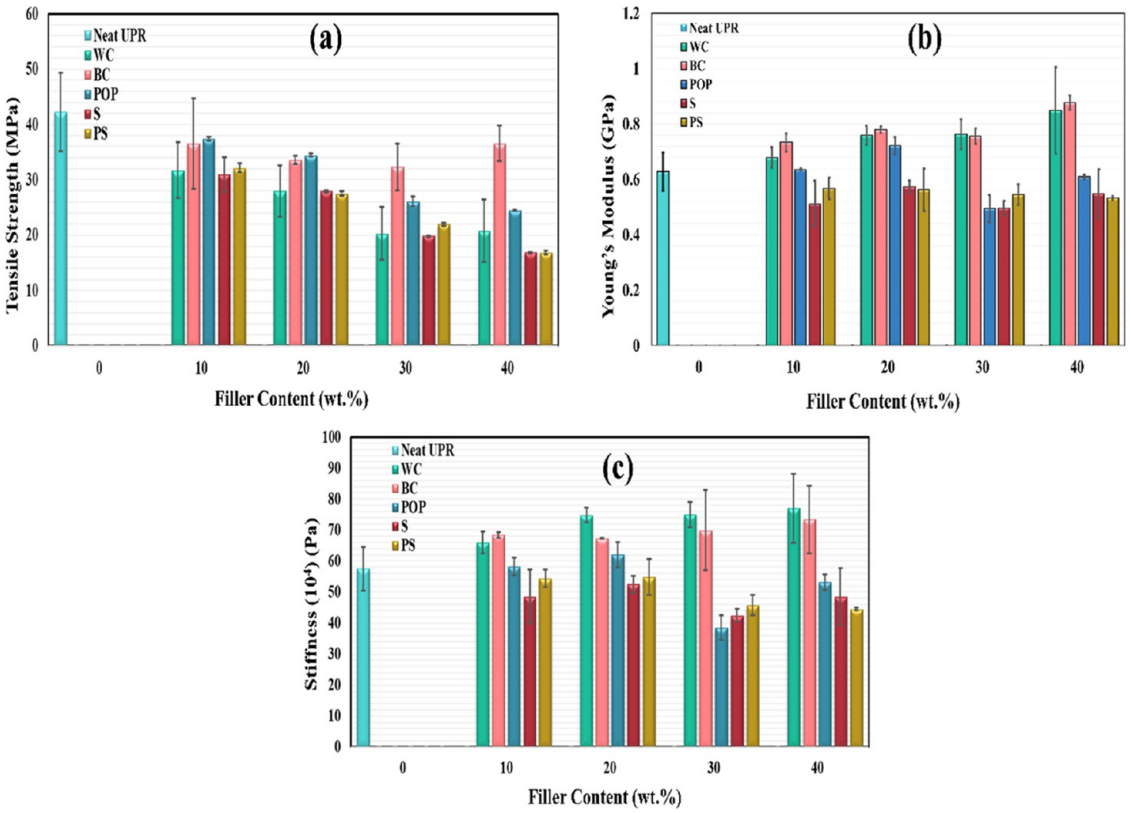

Figure 5. Tensile properties of UPR and cement polymer composites with different ratios: (a) tensile strength; (b) Young's modulus; (c) stiffness.

Table 2. Tensile Strength of Cement Polymer Composites (CPCs)

	tensile strength, MPa					
filler, wt %	neat UPR	WC	BC	POP	S	PS
0	42.25					
10		31.75	36.54	37.41	30.93	32.14
20		27.97	33.57	34.46	27.94	27.54
30		20.30	32.34	26.12	19.81	21.98
40		20.81	36.56	24.49	16.81	16.84

Table 3. Tensile Young's Modulus of Cement Polymer Composites (CPCs)

	Young's modulus, GPa					
filler, wt %	neat UPR	WC	BC	POP	S	PS
0	0.63					
10		0.68	0.73	0.64	0.51	0.57
20		0.76	0.78	0.72	0.57	0.56
30		0.76	0.76	0.50	0.50	0.55
40		0.85	0.88	0.61	0.55	0.53

Table 4. Tensile Stiffness of Cement Polymer Composites (CPCs)

	stiffness × 10^4, Pa					
filler, wt %	neat UPR	WC	BC	POP	S	PS
0	57.43					
10		66.01	68.41	58.38	48.59	54.41
20		74.83	67.36	62.06	52.58	54.89
30		74.97	69.95	38.51	42.49	45.89
40		76.99	73.39	53.22	48.52	44.47

is essential to consider the properties of the individual components and their interactions to optimize the stiffness of UPR/BC composites.

The stiffness of neat UPR and CPCs with different ratios of fillers are depicted in Figure 5c. Stiffness values for all fabricated specimens are recorded in Table 4. We observed that the stiffness values of UPR/S and UPR/PS composites were lower at different filler ratios (from 10 to 40 wt %) as compared to the value of neat UPR (57.433×10^4 Pa). The UPR/POP composite showed an unsystematic variation in stiffness values (see Table 4), in which the UPR/POP composite had higher stiffness values with filler ratios of 10 and 20 wt % as compared to the stiffness value of neat UPR and lower values at 30 and 40 wt % filler contents (see Figure 5c). The measured stiffness values of UPR/WC and UPR/BC composites with addition of different percentages of fillers (10−40 wt %) were found to be higher than those of neat UPR and UPR/POP composites. The UPR/WC and UPR/BC composites with higher aspect ratios of fillers ensure higher stiffness due to good compatibility and bonding between WC/BC particles and the resin (UPR).

3.1.2. Flexural Properties. The tests of flexural properties of the specimens were performed at a constant strain rate of 5 mm/min. The results of flexural strength of control (neat UPR) and CPCs with different filler ratios are shown in Figure 6. The correlations among the experimental maximum bending stress at break to introduce the different filler contents for enhancing the mechanical properties are shown in Figure 6a and Table 5. The mean values of maximal flexural strengths of UPR/WC, UPR/BC, UPR/POP, UPR/S, and UPR/PS composites were less than that of the resin (UPR). From Figure 6a, it could be seen that the CPCs showed an unsystematic change in flexural strength results. Among the polymer composite specimens, the results show that the UPR/WC composite exhibited better

https://doi.org/10.1021/acsomega.3c00353
ACS Omega 2023, 8, 20389−20403

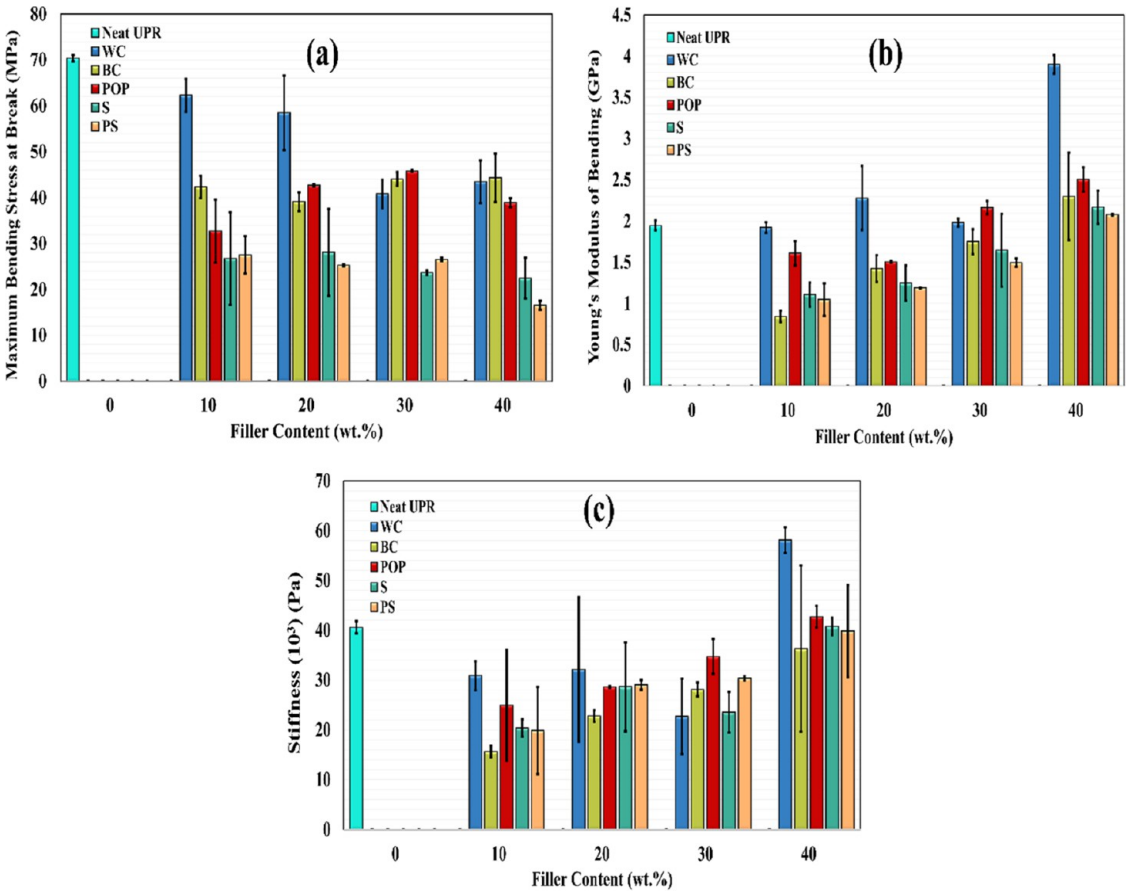

Figure 6. Flexural properties of UPR and cement polymer composites with different ratios: (a) maximum bending stress at break; (b) Young's modulus; and (c) stiffness.

Table 5. Flexural Strength of Cement Polymer Composites (CPCs)

	maximum bending stress at break, MPa					
filler, wt %	neat UPR	WC	BC	POP	S	PS
0	70.34					
10		62.31	42.35	32.72	26.75	27.51
20		58.49	39.15	42.67	28.10	25.29
30		40.85	44.05	45.78	23.67	26.53
40		43.49	44.31	38.93	22.46	16.58

Table 6. Flexural Young's Modulus of Cement Polymer Composites (CPCs)

	Young's modulus of bending, GPa					
filler, wt %	neat UPR	WC	BC	POP	S	PS
0	1.95					
10		1.92	0.84	1.61	1.11	1.05
20		2.28	1.42	1.51	1.25	1.19
30		1.98	1.75	2.16	1.65	1.50
40		3.90	2.30	2.51	2.17	2.08

flexural strength than UPR/BC, UPR/POP, UPR/S, and UPR/PS composites, whereas the highest value of flexural strength was observed to be 62.312 MPa at 10% WC filler loading, which resulted from the increased resistance to the chain of the polymer (UPR). Due to the poor interaction bonding between the matrix (UPR) and fillers (S and PS) (see SEM images), UPR/S and UPR/PS composites showed lower flexural strength

Table 7. Flexural Stiffness of Cement Polymer Composites (CPCs)

	stiffness × 10^3, Pa					
filler, wt %	neat UPR	WC	BC	POP	S	PS
0	40.56					
10		30.88	15.65	24.95	20.36	19.85
20		32.10	22.79	28.59	28.62	29.01
30		22.68	28.10	34.72	23.52	30.36
40		58.07	36.28	42.70	40.73	39.81

values (22.460−28.101 and 16.582−27.514 MPa, respectively) as compared to the other specimens of composites (see Table 5).

The flexural modulus of the test specimens is depicted in Figure 6b. The measured and calculated values of Young's modulus of bending for UPR/BC, UPR/POP, UPR/S, and UPR/PS composites were increased with increasing filler ratios systematically. It can be observed from Figure 6b that UPR/POP, UPR/S, and UPR/PS composites exhibited higher values of flexural modulus at 30 and 40 wt % fillers and the UPR/BC composite at 40 wt % BC as compared to UPR. At 40 wt % WC, UPR/WC showed the highest value (3.899 GPa) of Young's modulus of bending among all CPCs, as recorded in Table 6.

It is noted that the bending stiffness values in Figure 6c for UPR/BC, UPR/POP, and UPR/PS composites were increased with the increase in the filler ratio (BC, POP, and PS). The calculated bending stiffness values of UPR/WC, UPR/POP, and UPR/S composites at 40 wt % were higher than the values of

https://doi.org/10.1021/acsomega.3c00353
ACS Omega 2023, 8, 20389−20403

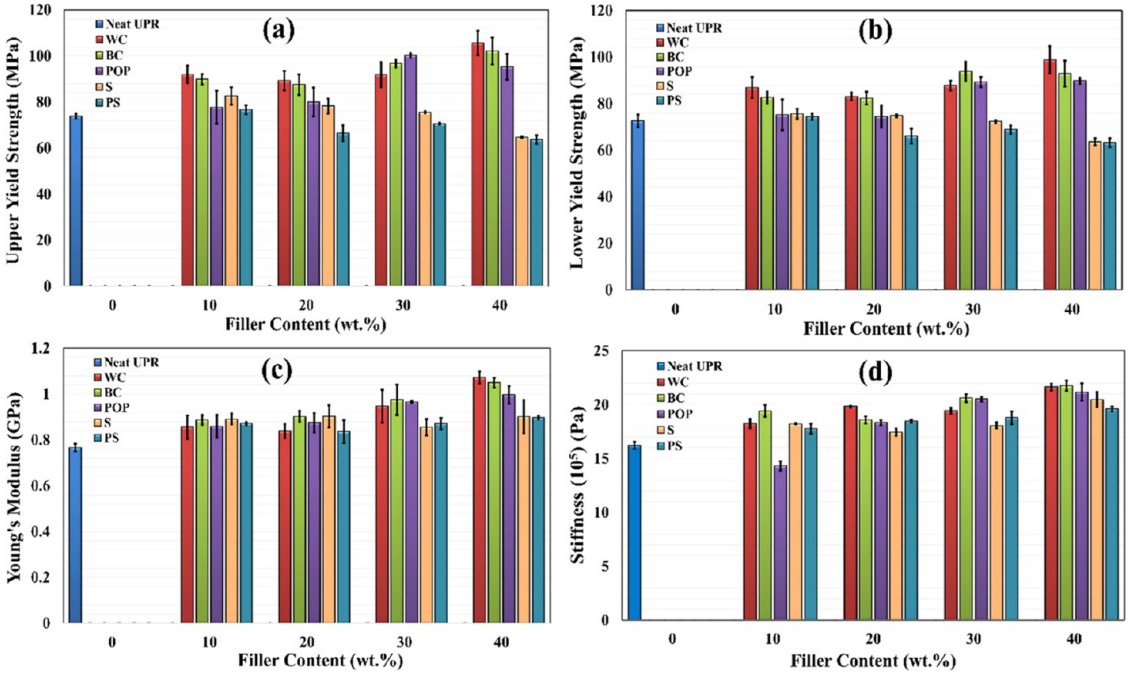

Figure 7. Compressive properties of UPR and cement polymer composites with different ratios: (a) upper yield strength; (b) lower yield strength; (c) Young's modulus; and (d) stiffness.

Table 8. Compressive Upper Yield Strength of Cement Polymer Composites (CPCs)

	upper yield strength, MPa					
filler, wt %	neat UPR	WC	BC	POP	S	PS
0	73.88					
10		92.00	89.87	77.74	82.61	76.65
20		89.25	87.51	79.93	78.22	66.47
30		91.88	96.73	100.26	75.50	70.52
40		105.69	102.13	95.25	64.67	63.70

Table 9. Compressive Lower Yield Strength of Cement Polymer Composites (CPCs)

	lower yield strength, MPa					
filler, wt %	neat UPR	WC	BC	POP	S	PS
0	72.62					
10		86.92	82.71	75.19	75.68	74.40
20		83.09	82.37	74.48	74.83	66.10
30		87.77	93.86	89.31	72.34	68.87
40		98.85	92.92	89.81	63.58	63.20

flexural stiffness for the matrix (UPR) (see Table 7). The measured results showed that the highest flexural stiffness value was found to be 58.065 × 10^3 Pa with the addition of 40 wt % WC in the UPR resin, which can further promote better interaction with the polymer.

3.1.3. Compressive Properties. The upper and lower yield strengths of UPR and CPCs were carried out by compression tests. We performed compressive testing of these samples and pristine UPR for comparison. For measuring the compressive properties, the testing speed has to be 5 mm/min. Figure 7a,b elucidates that the results of upper yield stress of all test specimens at different ratios are much higher than its lower yield strength. Yield strength indicates the maximum stress or load that a CPC specimen can withstand when it is deformed within its elastic limit. From Figure 7a, it could be seen that the results of upper yield strength for UPR/WC, UPR/BC, and UPR/POP composites with different percentages of fillers exhibited higher values than the UPR resin. This work suggested that the filler ratios of WC, BC, and POP in the UPR matrix not only could serve to suppress the grain growth but also could help improve the compressive yield strength and hardness of composite specimens. At 40 wt % S, the upper yield strength of UPR/S showed a small value, while UPR/PS displayed lower values at

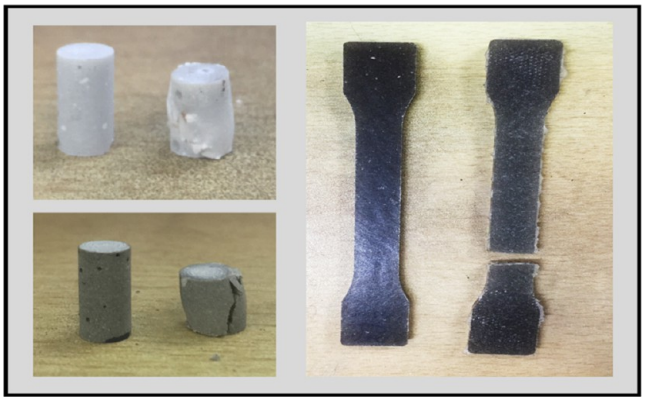

Figure 8. Image of fracture specimens.

Table 10. Compressive Young's Modulus of Cement Polymer Composites (CPCs)

	Young's modulus, GPa					
filler, wt %	neat UPR	WC	BC	POP	S	PS
0	0.77					
10		0.86	0.89	0.86	0.89	0.87
20		0.84	0.90	0.88	0.90	0.84
30		0.95	0.98	0.97	0.86	0.87
40		1.07	1.05	1.00	0.90	0.90

https://doi.org/10.1021/acsomega.3c00353
ACS Omega 2023, 8, 20389−20403

Table 11. Compressive Stiffness of Cement Polymer Composites (CPCs)

	stiffness × 10^5, Pa					
filler, wt %	neat UPR	WC	BC	POP	S	PS
0	16.23					
10		18.24	19.43	14.33	18.22	17.78
20		19.83	18.59	18.34	17.44	18.46
30		19.45	20.61	20.52	18.07	18.79
40		21.64	21.77	21.17	20.49	19.60

Table 12. Impact Strength of Cement Polymer Composites (CPCs)

	impact strength, kJ/m^2					
filler, wt %	neat UPR	WC	BC	POP	S	PS
0	14.37					
10		2.83	6.16	5.49	5.89	2.92
20		4.04	3.59	11.74	5.21	3.13
30		2.05	5.63	5.41	4.73	4.15
40		7.19	5.26	5.27	3.59	3.83

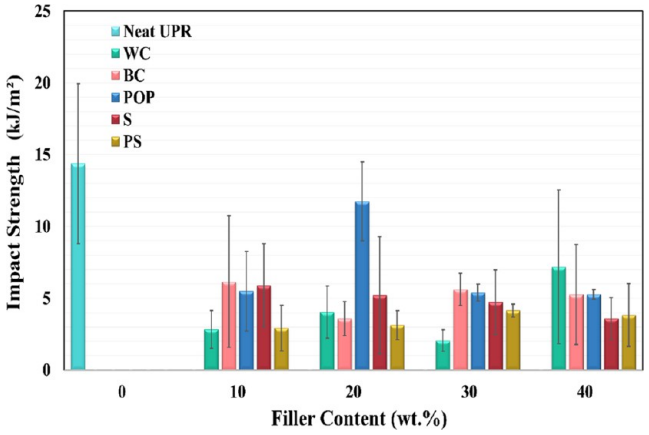

Figure 9. Impact strength properties of UPR and cement polymer composites with different ratios.

20, 30, and 40 wt % PS as compared to the reference matrix (UPR) and UPR/WC, UPR/BC, and UPR/POP composites, as tabulated in Table 8. This result could be due to restriction of mobility of polyester chains by S and PS, causing a relatively weak matrix interface. The highest value of the compressive upper yield strength was measured to be 105.687 MPa with loading 40 wt % WC in the UPR matrix (see Figure 7a and Table 8). Figure 7b illustrates the compressive lower yield strength of the compressive test. The result showed that the experimentally determined values of the compressive lower yield strength for UPR/WC, UPR/BC, and UPR/POP composites were higher than the reference matrix. UPR/S at 30 and 40 wt % S and UPR/PS at 20, 30, and 40 wt % showed lower yield strength values as compared to the reference matrix (UPR), UPR/WC, UPR/BC, and UPR/POP composites (see Figure 7b and Table 9). The compressive fracture surface of specimens is shown in Figure 8. Decrement in the lower yield strength values of UPR/S and UPR/PS (from 10 to 40 wt % fillers) could be the result of grain size variations of S and Ps and deformation structure in these composite specimens. These models of composite UPR/S and UPR/PS can account for the influence of porosity and filler grain size on the reduction of mechanical properties.

Table 13. Water Absorption of Cement Polymer Composites (CPCs)

	water absorption, %				
sample ID	1 week	2 weeks	3 weeks	4 weeks	5 weeks
neat UPR	0.16	0.48	0.73	0.89	1.06
UPR/WC-10	0.72	1.27	2.46	3.56	3.74
UPR/WC-20	1.57	2.20	3.04	3.23	3.31
UPR/WC-30	1.80	2.13	2.13	2.30	2.47
UPR/WC-40	1.74	2.21	2.41	2.68	3.09
UPR/BC-10	1.23	1.98	4.30	5.96	6.20
UPR/BC-20	0.94	1.58	3.72	4.75	5.07
UPR/BC-30	1.38	1.95	3.75	4.11	4.11
UPR/BC-40	1.83	2.46	2.94	3.50	3.70
UPR/POP-10	0.72	0.87	1.71	2.09	2.16
UPR/POP-20	0.73	0.87	1.91	2.13	2.38
UPR/POP-30	0.57	0.97	2.05	2.66	2.83
UPR/POP-40	0.42	0.96	2.36	3.50	3.60
UPR/S-10	0.54	0.70	1.27	1.52	1.76
UPR/S-20	0.61	0.75	1.29	1.43	1.84
UPR/S-30	0.65	0.87	1.62	2.29	2.52
UPR/S-40	0.61	0.68	1.37	2.13	2.20
UPR/PS-10	0.89	1.18	1.40	1.92	2.21
UPR/PS-20	0.88	1.02	1.24	1.60	1.78
UPR/PS-30	0.88	1.23	1.44	2.08	2.22
UPR/PS-40	0.97	1.24	1.64	2.20	2.32

The variations of CPC modulus with respect to filler ratios are depicted in Figure 7c. From this figure, it is found that at all different filler ratios, the compressive Young's moduli of the composites are always higher than those of the matrix (see Table 10). Compressive Young's moduli of UPR/WC, UPR/BC, and UPR/POP composites were found to increase with the filler content (from 10 to 40 wt %). At 40 wt %, the highest values of compressive Young's modulus for both specimens of UPR/WC and UPR/BC were found to be nearly the same (1.072 and 1.049 GPa, respectively), as seen in Table 10. The values of Young's modulus for UPR/S were varied from 0.856 to 0.903 GPa, and the values of the compressive modulus of UPR/PS were varied from 0.836 to 0.897 GPa. The variations in UPR/S and UPR/S composite values could be attributed to the combination of the filler and the polymer and the ability of the S and PS ratio to deform the polymer matrix.

Figure 7d illustrates the compressive stiffness of CPCs with respect to different filler ratios. The measured results of CPCs showed the improved compressive stiffness with the loading fillers in the UPR matrix (see Figure 7d). The altered stiffness in composites is attributed to the particle size of fillers and the dispersion of fillers in the matrix.[40] It is also inferred to be due to the higher stiffness of the added filler, which imparts its property to the weaker matrix and reinforcement. The analysis of compressive stiffness properties showed that the best result belonged to the test specimens made of WC/UPR and BC/UPR, in which the highest stiffness was observed at 40 wt % BC (21.767 × 10^5 Pa). It can be seen from Table 11 that WC/UPR and BC/UPR have close values of stiffness (21.644 × 10^5, 21.767 × 10^5 Pa) at 40 wt % fillers. The lowest compressive stiffness value (14.333 × 10^5 Pa) among the test specimens was observed for POP/UPR at 10 wt % POP (see Table 11).

3.1.4. Impact Properties. The impact test was carried out for characterization of composites by the Izod/Charpy impact tester, and the results were recorded and are shown in Table 12. The results of the present work have shown that the measured

https://doi.org/10.1021/acsomega.3c00353
ACS Omega 2023, 8, 20389−20403

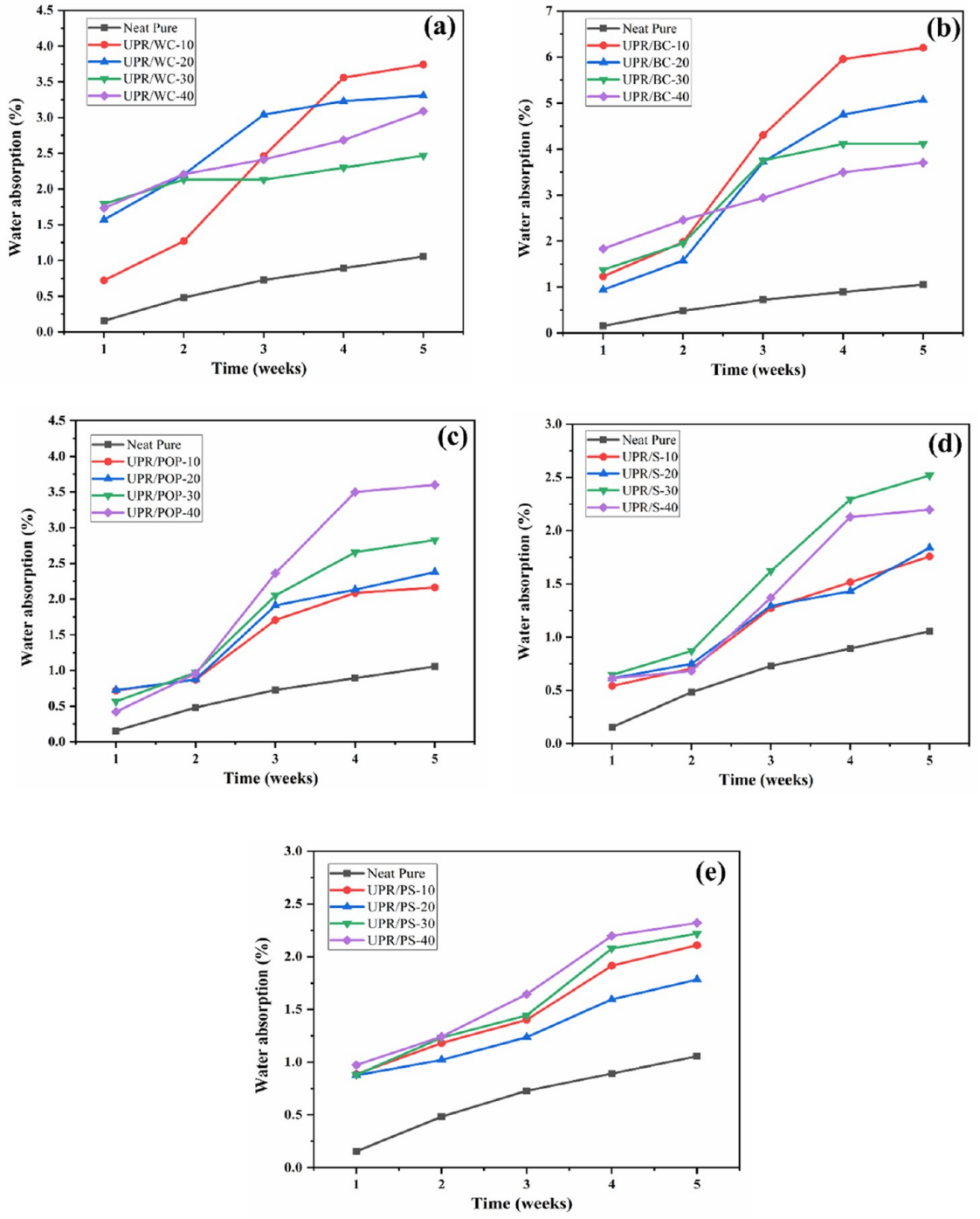

Figure 10. Water absorption of the UPR and cement polymer composite specimens with different ratios: (a) UPR/WC (b) UPR/BC (c) UPR/POP (d) UPR/S, and (e) UPR/PS.

impact strengths for all cement composite specimens were lower than those of the reference UPR, as can be seen in Figure 9. The impact strengths of UPR/S values decreased on increasing the filler ratio of S. Generally, the lower impact strength of composite specimens showed that the material is incapable of resisting sudden or high load. Among the CPCs, the UPR/POP composite showed the highest strength at 20 wt % POP (11.743 kJ/m^2), while the lowest impact strength was observed with the addition 20 wt % WC in the UPR matrix, which was found to be 2.053 kJ/m^2, as shown in Figure 9 and recorded in Table 12. The variation in the results of impact strength for CPCs might be ascribed to the polymer structure of UPR, the combination of UPR with the fillers, the structure of composite specimens, and the microcracks in the composites.

3.2. Water Absorption. Typically, composite durability is attributed to its capability to water absorption resistance. The water absorption test of CPCs was performed as referred to in the ASTM D570-98 standard. The percentage of water absorption in the CPCs was calculated by the weight difference between the specimens immersed in distilled water and the dry specimens.

https://doi.org/10.1021/acsomega.3c00353
ACS Omega 2023, 8, 20389−20403

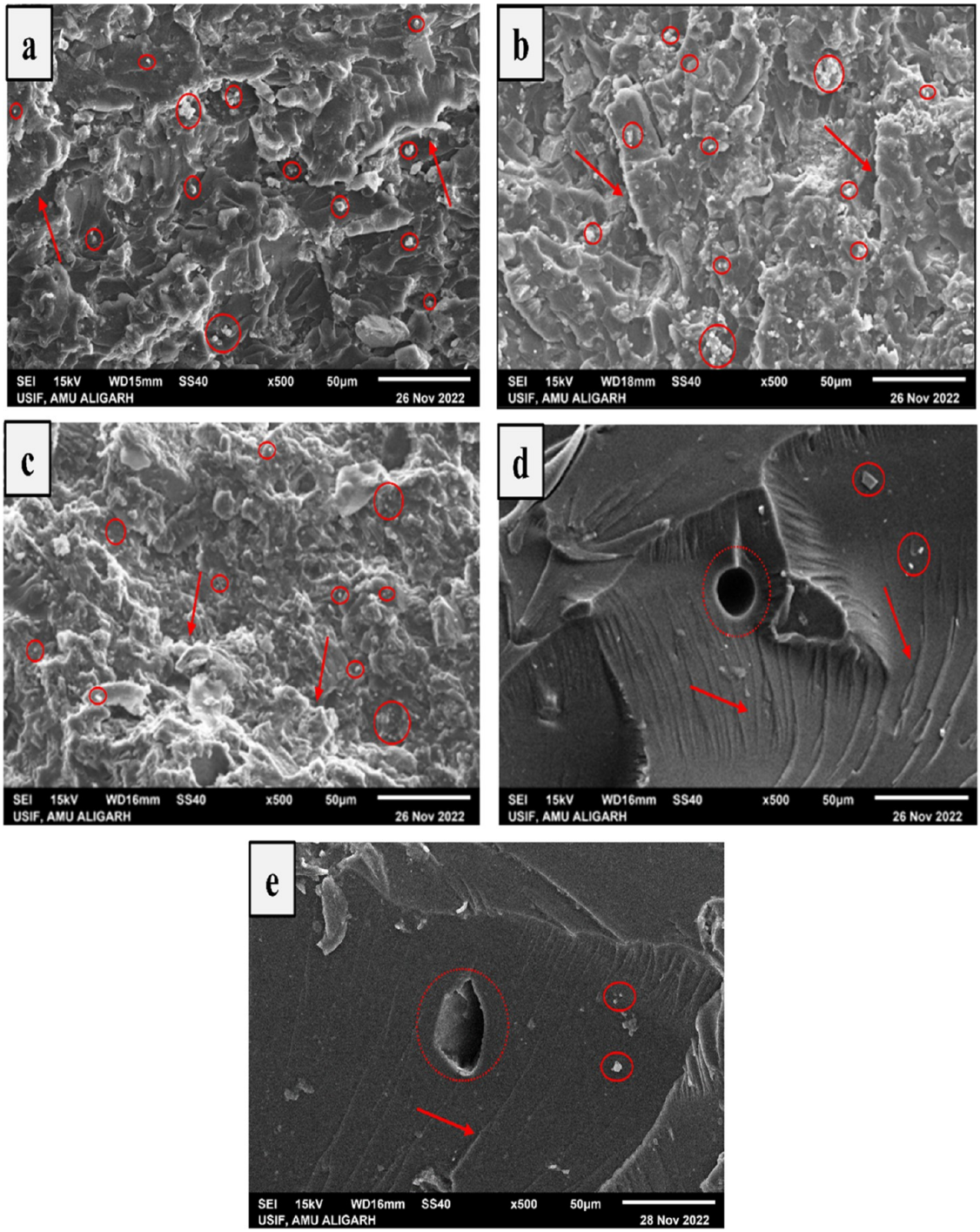

Figure 11. SEM of the fracture surface: (a) UPR/WC; (b) UPR/BC; (c) UPR/POP; (d) UPR/S; (e) UPR/PS. In addition, the red solid circles in SEM images of (a), (b), and (c) highlight good dispersion of filler particles and poor dispersion in images (d) and (e); red arrows in images (a), (b), and (c) indicate the UPR surface. The red dotted circles and arrows in images (d) and (e) indicate the bordering lacuna and propagation of cracks, respectively.

Water absorption was calculated by the following equation[41,42]

$$\text{water absorption } (\%) = \frac{M_w - M_d}{M_d} \times 100$$

where M_w and M_d are the wet weight and dry weight of the sample, respectively.

The calculation results are summarized in Table 13.

Figure 10a–d shows the percentage of water absorption for all of the CPC specimens. The rate of water absorption gradually increased until it reached the saturation point or the maximum water gain value of the CPCs. We note that the percentage of water absorption CPCs varies from 1.76 to 6.702% during the period of immersion estimated at 5 weeks. It is worth noting that the absorption capacity of CPCs decreased in the following order: UPR/BC > UPR/WC > UPR/POP > UPR/PS > UPR/S. As observed from Figure 10, the water penetrated the CPC

https://doi.org/10.1021/acsomega.3c00353
ACS Omega 2023, 8, 20389−20403

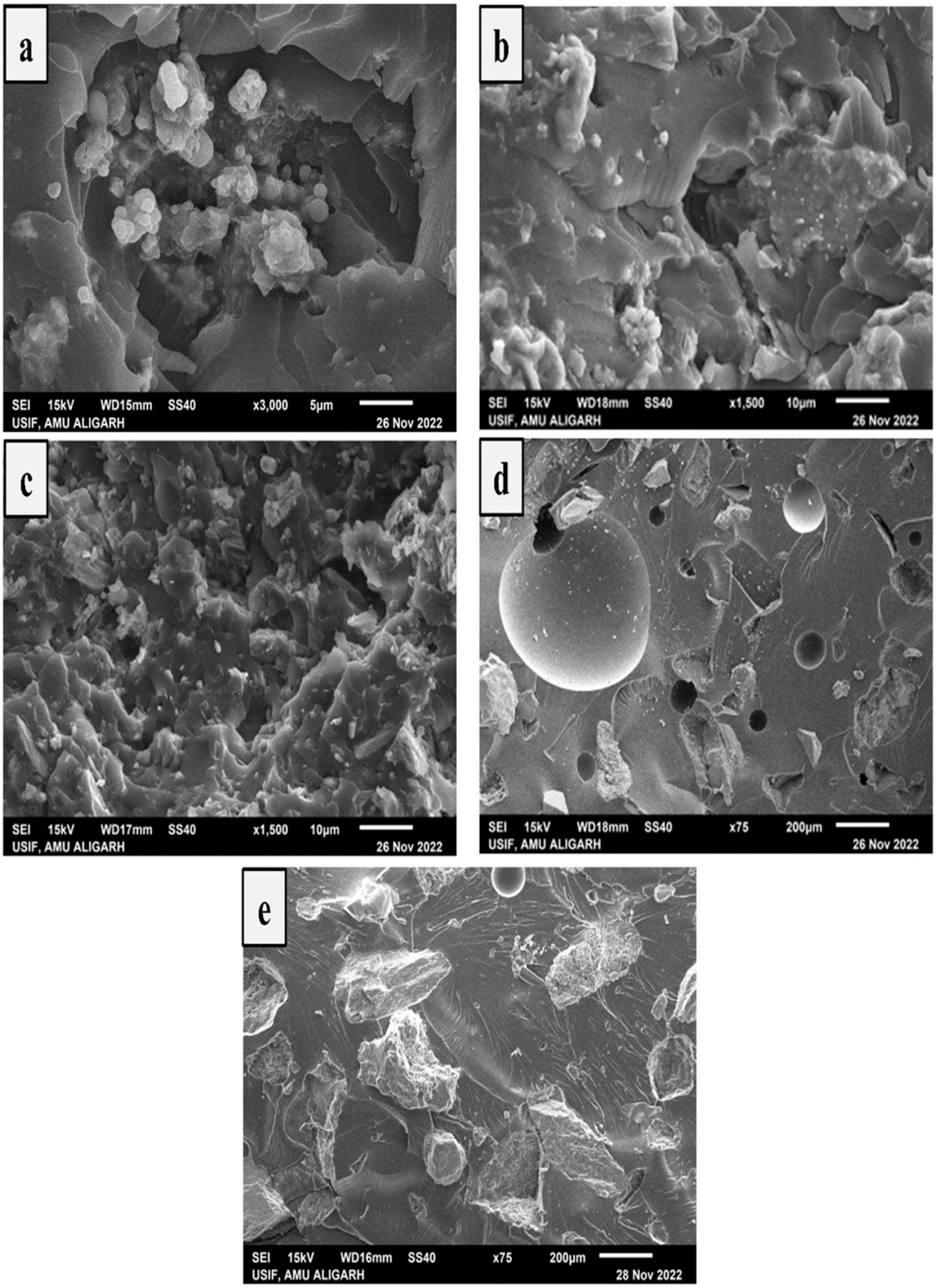

Figure 12. SEM of the fracture surface: (a) UPR/WC; (b) UPR/BC; (c) UPR/POP; (d) UPR/S; and (e) UPR/PS.

specimens abruptly in the first 3 weeks and then gradually slowed down when reaching the 4th week of immersion. The water uptake reached equilibrium between 4 and 5 weeks.

From Table 13, the highest percentages of water absorption were 6.202 and 5.07% for UPR/BC-10 and UPR/BC-20, while the lowest percentages of water absorption were 1.76 and 1.84% for UPR/S-10 and UPR/S-20, respectively. The water penetrates the CPCs due to the good compatibility among BC, WC, POP, and water as well as microgaps and microcracks in the surface of the composite[43−45] (see Figures 11 and 12).

3.3. Morphology of Cement Polymer Composites (CPCs). The mechanical properties of CPCs of UPR/WC, UPR/BC, UPR/POP, UPR/S, and UPR/PS are determined by their microstructure. In order to understand the relationship

https://doi.org/10.1021/acsomega.3c00353
ACS Omega 2023, 8, 20389−20403

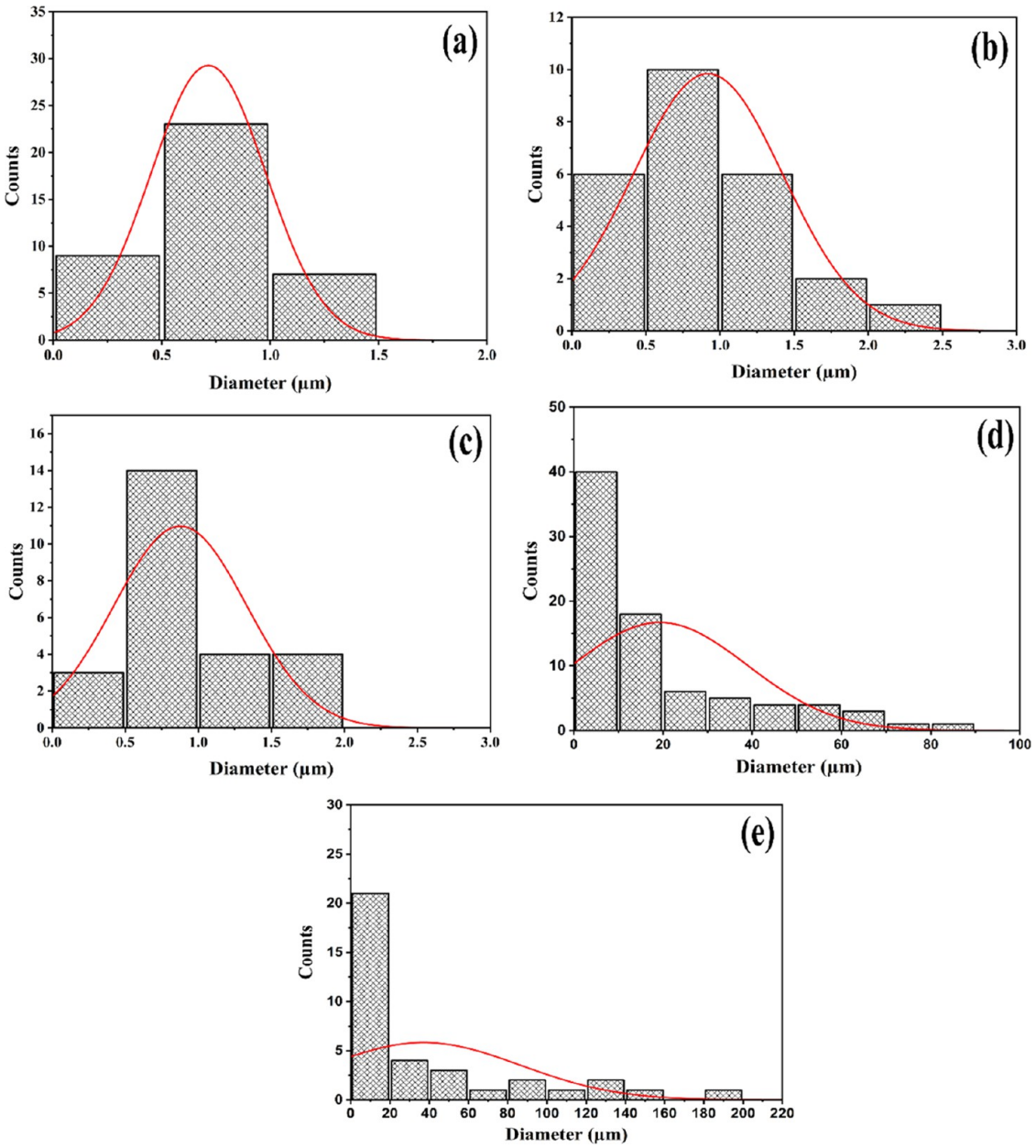

Figure 13. Particle size distribution determined from SEM images: (a) WC; (b) BC; (c) POP; (d) S; and (e) PS.

Table 14. Particle Size Values of Cementitious Materials

filler	minimum particle size (μm)	maximum particle size (μm)	mean particle size (μm)
WC	0.179	1.217	0.71
BC	0.354	2.193	0.92
POP	0.349	1.77	0.88
S	1.839	192.149	37.11
PS	2.049	82.643	18.66

between the mechanical strength and microstructure of the CPCs, the corresponding SEM images of manufactured specimens were also investigated. Morphologies of the fracture surface of the polymer/cement composite (UPR/filler (70/30)) are shown in Figure 11. From Figure 11a−c, it can be seen that the particulate matter is more evenly dispersed in the UPR/WC, UPR/BC, and UPR/POP matrixes, indicating that the incorporation of WC, BC, and POP fillers in the UPR resin matrix can effectively prevent microcracks from further propagating during the fracture of the matrix. With good dispersion and distribution of cement particles in the polymer matrix, the CPCs can help and play a key role in strengthening and toughening effects. The fracture surfaces of UPR/S and UPR/PS composites are shown in Figure 11d,e; it can be observed from images d and e that the cross-section morphologies of UPR/S and UPR/PS composites exhibited a dimple in the middle of the fracture surface and led to propagation of cracks. During the test of mechanical properties, the pores are likely to cause crack growth; thus, the strength of the composite specimens decreases significantly.

From the enlarged photo in Figure 12a,b, SEM images revealed the presence of microcracks on the surfaces of UPR/WC and UPR/BC composites. A microcrack can be clearly seen in the surrounding region of the agglomeration of filler particles (particle clusters). Figure 12c shows good dispersion and less/no agglomeration of filler particles on the composite surface of

https://doi.org/10.1021/acsomega.3c00353
ACS Omega 2023, 8, 20389−20403

the UPR/POP composite. As the filler particles were dispersed, the CPCs obtained good mechanical properties. The fracture surface morphologies of UPR/WC, UPR/WC, and UPR/POP composites indicate relatively less matrix deformation and few microcracks, which could be the result of agglomerates present in these composite matrixes. Figure 12d,e shows the fracture surfaces of UPR/S and UPR/PS. Analyzing Figure 12d,e, it was observed poor dispersion of fillers particles in the UPR matrix, large particles, propagation of cracks, and the presence of pull-out. The fracture surface appearance of UPR/S and UPR/PS includes a concave surface, voids, and lacuna (dimples), which could lead to reductions in the mechanical strength of composite specimens, as shown in Figure 12d,e. During the mechanical test, the pores are likely to cause crack growth; thus, the strength of the composite material decreases significantly. The large particles of S and PS interaction with the polymer matrix resulted in poor dispersion of filler particles and consequently reduced the microhardness.

The maximum probability of particle size distribution can be determined using the mathematical model (Gaussian curvature) depicted in Figure 13a−e. The particle size of cementitious material-filled unsaturated polyester resin composites is an important parameter that influences the mechanical and physical properties of the resulting composites. Table 14 displays the minimum, maximum, and average particle sizes of the fillers. The average particle size (μm) of fillers, from smallest to largest, is as follows: WC (0.71), POP (0.88), BC (0.92), S (18.66), and PS (37.11). Although WC particles are smaller than POP, UPR/POP composites exhibit the highest tensile strength. SEM images indicate that UPR/WC composites display agglomeration, which leads to decreased mechanical properties. In contrast, UPR/POP composites exhibit little or no agglomeration, resulting in good tensile strength. S and PS fillers have large particle sizes that explain the lowest mechanical properties in the UPR/S and UPR/PS composites. The lower mechanical properties observed in the UPR/S and UPR/PS composites can be attributed to the large particle sizes of the S and PS fillers.

4. CONCLUSIONS AND SUGGESTIONS

The present investigation examined the effect of different filler ratios on the mechanical behavior of cement polymer composites. The results show that the mechanical properties, such as tensile, flexural, compressive, and impact strength, of the composites are greatly influenced by the filler nature and content. Specifically, the loading of CM led to a decrease in the tensile, flexural, and impact strengths of CPCs. However, the effect on Young's modulus and stiffness was inconsistent, with some CM fillers leading to an increase and others to a decrease compared to the control (neat UPR). In contrast, the upper and lower yield strengths of WC, BC, and POP in UPR filled with 10−40 wt % of these fillers increased compared to the control. Furthermore, the compressive Young's modulus of all CM fillers was higher than that of neat UPR, and the compressive stiffness was higher for all CM fillers except for POP at 10 wt %. The mechanical behavior results of UPR/WC, UPR/BC, and UPR/POP composites confirm that the loading of these fillers in the UPR matrix provides better reinforcement compared to UPR/S and UPR/PS composites. This study concluded that the mechanical properties of CPCs can be affected by various factors, such as filler particle size and distribution and the presence of microcracks. The loading of CM led to an increase in water absorption of CPCs, while UPR/S and UPR/PS composites exhibited significantly greater water resistance compared to other composites. The increase in water absorption of CPCs resulting from the loading of CM was attributed to the good compatibility among BC, WC, POP, and water, as well as the presence of microgaps and microcracks on the surface of the composite. In contrast, UPR/S and UPR/PS composites showed superior water resistance compared to other composites. In sum, our results showed clearly that the enhancement of mechanical properties of these composite materials was due to cementitious material's nature and structure and its behavior in the resin matrix. Accordingly, we suggest UPR/WC, UPR/BC, and UPR/POP composite materials as a class of advanced materials that can be used in constructions and to repair large cracks, while UPR/S and UPR/PS coatings can be used to protect cracked and water absorption resistance. Our finding indicates the need for further research to prepare hybrid cementitious material fillers/UPR composites in terms of construction and diverse applications.

■ ASSOCIATED CONTENT

Data Availability Statement

All of the findings of this study and supporting data are available from the authors upon request.

■ AUTHOR INFORMATION

Corresponding Authors

Salah M. S. Al-Mufti − *Department of Petroleum Studies, Z. H. College of Engineering & Technology, Aligarh Muslim University, Aligarh 202002, India;* orcid.org/0000-0001-9084-8897; Email: smo995238@gmail.com

Syed J. A. Rizvi − *Department of Petroleum Studies, Z. H. College of Engineering & Technology, Aligarh Muslim University, Aligarh 202002, India*; Phone: +91-9557413925; Email: sjarizvi@zhcet.ac.in

Author

Asma Almontasser − *Department of Applied Physics, Z. H. College of Engineering & Technology, Aligarh Muslim University, Aligarh 202002, India*

Complete contact information is available at: https://pubs.acs.org/10.1021/acsomega.3c00353

Author Contributions

S.M.S.A.-M. and S.J.A.R. designed the study. S.M.S.A.-M. performed the experiments and measurements and analyzed the results. S.M.S.A.-M. and A.A. wrote the paper. A.A. conceptualized the manuscript, performed the SEM analysis, and analyzed the overall results. S.J.A.R. analyzed the results and reviewed and edited the manuscript. All authors were involved in the evaluation of results. All authors have reviewed and agreed to publish the final version of the manuscript.

Notes

The authors declare no competing financial interest.

■ ACKNOWLEDGMENTS

The authors are thankful to the National Small Industries Corporation Ltd., Aligarh, India, and the Department of Civil Engineering, Aligarh Muslim University, Aligarh, India, for the generous help.

■ REFERENCES

(1) Al-Mufti, S. M. S.; Almontasser, A.; Rizvi, S. J. A. Single and Double Thermal Reduction Processes for Synthesis Reduced Graphene

Oxide Assisted by a Muffle Furnace: A Facile Robust Synthesis and Rapid Approach to Enhance Electrical Conductivity. *AIP Adv.* **2022**, *12*, No. 125306.
(2) Chen, Z.-s.; Zhou, X.; Wang, X.; Guo, P. Mechanical Behavior of Multilayer GO Carbon-Fiber Cement Composites. *Constr. Build. Mater.* **2018**, *159*, 205−212.
(3) Wang, J.; Dong, S.; Yu, X.; Han, B. Mechanical Properties of Graphene-Reinforced Reactive Powder Concrete at Different Strain Rates. *J. Mater. Sci.* **2020**, *55*, 3369−3387.
(4) Douba, A.; Emiroglu, M.; Kandil, U. F.; Taha, M. M. R. Very Ductile Polymer Concrete Using Carbon Nanotubes. *Constr. Build. Mater.* **2019**, *196*, 468−477.
(5) Reddy, P. V. R. K.; Prasad, D. R. Investigation on the Impact of Graphene Oxide on Microstructure and Mechanical Behaviour of Concrete. *J. Build. Pathol. Rehabil.* **2022**, *7*, 30.
(6) Rehman, S. K. U.; Ibrahim, Z.; Jameel, M.; Memon, S. A.; Javed, M. F.; Aslam, M.; Mehmood, K.; Nazar, S. Assessment of Rheological and Piezoresistive Properties of Graphene Based Cement Composites. *Int. J. Concr. Struct. Mater.* **2018**, *12*, 64.
(7) Belyakov, A. V. Carbon Nanotubes for the Synthesis of Ceramic Matrix Composites (Cleaning, Dispersion, Surface Modification) (Review). *Refract. Ind. Ceram.* **2019**, *60*, 92−100.
(8) Zhou, K.; Li, W.; Patel, B. B.; Tao, R.; Chang, Y.; Fan, S.; Diao, Y.; Cai, L. Three-Dimensional Printable Nanoporous Polymer Matrix Composites for Daytime Radiative Cooling. *Nano Lett.* **2021**, *21*, 1493−1499.
(9) Ji, S.-Y.; Jung, H.-B.; Kim, M.-K.; Lim, J.-H.; Kim, J.-Y.; Ryu, J.; Jeong, D.-Y. Enhanced Energy Storage Performance of Polymer/Ceramic/Metal Composites by Increase of Thermal Conductivity and Coulomb-Blockade Effect. *ACS Appl. Mater. Interfaces* **2021**, *13*, 27343−27352.
(10) Zhao, L.; Lee, T.; Ryu, S.; Oshima, Y.; Guo, Q.; Zhang, D. Mechanical Robustness of Metal Nanocomposites Rendered by Graphene Functionalization. *Nano Lett.* **2021**, *21*, 5706−5713.
(11) Tran, B. N.; Thickett, S. C.; Agarwal, V.; Zetterlund, P. B. Influence of Polymer Matrix on Polymer/Graphene Oxide Nanocomposite Intrinsic Properties. *ACS Appl. Polym. Mater.* **2021**, *3*, 5145−5154.
(12) Praveena, B.; Shetty, B. P.; Sachin, B.; Yadav, S. P. S.; Avinash, L. Physical and Mechanical Properties, Morphological Behaviour of Pineapple Leaf Fibre Reinforced Polyester Resin Composites. *Adv. Mater. Process. Technol.* **2022**, *8*, 1147−1159.
(13) Rahman, M. M.; Islam, M. A. Application of Epoxy Resins in Building Materials: Progress and Prospects. *Polym. Bull.* **2022**, *79*, 1949−1975.
(14) Benmokrane, B.; Ali, A. H.; Mohamed, H. M.; ElSafty, A.; Manalo, A. Laboratory Assessment and Durability Performance of Vinyl-Ester, Polyester, and Epoxy Glass-FRP Bars for Concrete Structures. *Composites, Part B* **2017**, *114*, 163−174.
(15) Manalo, A.; Maranan, G.; Benmokrane, B.; Cousin, P.; Alajarmeh, O.; Ferdous, W.; Liang, R.; Hota, G. Comparative Durability of GFRP Composite Reinforcing Bars in Concrete and in Simulated Concrete Environments. *Cem. Concr. Compos.* **2020**, *109*, No. 103564.
(16) Somarathna, H. M. C. C.; Raman, S. N.; Mohotti, D.; Mutalib, A. A.; Badri, K. H. The Use of Polyurethane for Structural and Infrastructural Engineering Applications: A State-of-the-Art Review. *Constr. Build. Mater.* **2018**, *190*, 995−1014.
(17) Nodehi, M. Epoxy, Polyester and Vinyl Ester Based Polymer Concrete: A Review. *Innovative Infrastruct. Solutions* **2022**, *7*, 64.
(18) Józefiak, K.; Michalczyk, R. Prediction of Structural Performance of Vinyl Ester Polymer Concrete Using FEM Elasto-Plastic Model. *Materials* **2020**, *13*, 4034.
(19) Ferdous, W.; Manalo, A.; Wong, H. S.; Abousnina, R.; AlAjarmeh, O. S.; Zhuge, Y.; Schubel, P. Optimal Design for Epoxy Polymer Concrete Based on Mechanical Properties and Durability Aspects. *Constr. Build. Mater.* **2020**, *232*, No. 117229.
(20) Zhang, H.; Gao, Y.; Hong, J.; Li, C.; Kang, H.; Zhang, Z.; Huang, M. Laboratory Research on Road Performances of Unsaturated Polyester Concrete at Medium-High Temperature. *Constr. Build. Mater.* **2020**, *254*, No. 119318.
(21) Gao, Y.; romero, P.; Zhang, H.; Huang, M.; Lai, F. Unsaturated Polyester Resin Concrete: A Review. *Constr. Build. Mater.* **2019**, *228*, No. 116709.
(22) Marín, D.; Gañán, P.; Tercjak, A.; Castro, C.; Builes, D. H. Phase Distribution Changes of Neat Unsaturated Polyester Resin and Their Effects on Both Thermal Stability and Dynamic-Mechanical Properties. *J. Appl. Polym. Sci.* **2021**, *138*, 51308.
(23) Rajaee, P.; Ashenai Ghasemi, F.; Fasihi, M.; Saberian, M. Effect of Styrene-Butadiene Rubber and Fumed Silica Nano-Filler on the Microstructure and Mechanical Properties of Glass Fiber Reinforced Unsaturated Polyester Resin. *Composites, Part B* **2019**, *173*, No. 106803.
(24) Chen, Z.; Yu, Y.; Zhang, Q.; Chen, Z.; Chen, T.; Li, C.; Jiang, J. Surface-Modified Ammonium Polyphosphate with (3-Aminopropyl) Triethoxysilane, Pentaerythritol and Melamine Dramatically Improve Flame Retardancy and Thermal Stability of Unsaturated Polyester Resin. *J. Therm. Anal. Calorim.* **2021**, *143*, 3479−3488.
(25) Zhang, H.; Su, C.; Bu, X.; Zhang, Y.; Gao, Y.; Huang, M. Laboratory Investigation on the Properties of Polyurethane/Unsaturated Polyester Resin Modified Bituminous Mixture. *Constr. Build. Mater.* **2020**, *260*, No. 119865.
(26) Heriyanto; Pahlevani, F.; Sahajwalla, V. Effect of Different Waste Filler and Silane Coupling Agent on the Mechanical Properties of Powder-Resin Composite. *J. Cleaner Prod.* **2019**, *224*, 940−956.
(27) Chowaniec, A.; Czarnecki, S.; Sadowski, Ł. The Effect of the Amount and Particle Size of the Waste Quartz Powder on the Adhesive Properties of Epoxy Resin Coatings. *Int. J. Adhes. Adhes.* **2022**, *117*, No. 103009.
(28) Erkliğ, A.; Alsaadi, M.; Bulut, M. A Comparative Study on Industrial Waste Fillers Affecting Mechanical Properties of Polymer-Matrix Composites. *Mater. Res. Express* **2016**, *3*, No. 105302.
(29) Tabatabai, H.; Janbaz, M.; Nabizadeh, A. Mechanical and Thermo-Gravimetric Properties of Unsaturated Polyester Resin Blended with FGD Gypsum. *Constr. Build. Mater.* **2018**, *163*, 438−445.
(30) Ahmad, T.; Raza, S. S.; Aleem, E.; Kamran, M.; Manzoor, U.; Makhdoom, A.; Ahmad, R.; Mukhtar, S. Improvement in Mechanical and Thermal Properties of Unsaturated Polyester- Based Hybrid Composites. *Iran. Polym. J.* **2017**, *26*, 305−311.
(31) de Souza, L. G. M.; da Silva, E. J.; Meira de Souza, L. G. V. Obtaining and Characterizing a Polyester Resin and Cement Powder Composites. *Mater. Res.* **2020**, *23*, 1−8.
(32) Singer, G.; Sinn, G.; Schwendtner, K.; Lichtenegger, H. C.; Wan-Wendner, R. Time-Dependent Changes of Mechanical Properties of Polymer-Based Composite Materials for Adhesive Anchor Systems. *Compos. Struct.* **2018**, *196*, 155−162.
(33) Shettar, M.; Hiremath, P. Effect of Seawater on Mechanical Properties of GFRP with Cement as Filler Material for Fishing Boat Application. *Int. J. Appl. Eng. Res.* **2015**, *10*, 40027−40030.
(34) Raajeshkrishna, C. R.; Chandramohan, P. Effect of Reinforcements and Processing Method on Mechanical Properties of Glass and Basalt Epoxy Composites. *SN Appl. Sci.* **2020**, *2*, 959.
(35) Sanya, O. T.; Oji, B.; Owoeye, S. S.; Egbochie, E. J. Influence of Particle Size and Particle Loading on Mechanical Properties of Silicon Carbide−Reinforced Epoxy Composites. *Int. J. Adv. Manuf. Technol.* **2019**, *103*, 4787−4794.
(36) Guven, I.; Cinar, K. Micromechanical Modeling of Particulate-Filled Composites Using Micro-CT to Create Representative Volume Elements. *Int. J. Mech. Mater. Des.* **2019**, *15*, 695−714.
(37) Rizvi, S. J. A.; Bhatnagar, N. Microcellular PP vs. Microcellular PP/MMT Nanocomposites: A Comparative Study of Their Mechanical Behavior. *Int. Polym. Process.* **2011**, *26*, 375−382.
(38) Nilagiri Balasubramanian, K. B.; Ramesh, T. Role, Effect, and Influences of Micro and Nano-Fillers on Various Properties of Polymer Matrix Composites for Microelectronics: A Review. *Polym. Adv. Technol.* **2018**, *29*, 1568−1585.

https://doi.org/10.1021/acsomega.3c00353
ACS Omega 2023, 8, 20389−20403

(39) Samal, S. Effect of Shape and Size of Filler Particle on the Aggregation and Sedimentation Behavior of the Polymer Composite. *Powder Technol.* **2020**, *366*, 43−51.
(40) Fu, S.-Y.; Feng, X.-Q.; Lauke, B.; Mai, Y.-W. Effects of Particle Size, Particle/Matrix Interface Adhesion and Particle Loading on Mechanical Properties of Particulate−Polymer Composites. *Composites, Part B* **2008**, *39*, 933−961.
(41) Venkatesh, C.; Nerella, R.; Chand, M. S. R. Role of Red Mud as a Cementing Material in Concrete: A Comprehensive Study on Durability Behavior. *Innovative Infrastruct. Solutions* **2021**, *6*, 13.
(42) Wang, L.-l.; Dong, X.; Wang, X.; Zhu, G.; Li, H.; Wang, D. High Performance Long Chain Polyamide/Calcium Silicate Whisker Nanocomposites and the Effective Reinforcement Mechanism. *Chin. J. Polym. Sci.* **2016**, *34*, 991−1000.
(43) Alamri, H.; Low, I. M. Effect of Water Absorption on the Mechanical Properties of N-SiC Filled Recycled Cellulose Fibre Reinforced Epoxy Eco-Nanocomposites. *Polym. Test.* **2012**, *31*, 810−818.
(44) Hamdan, M. H. M.; Siregar, J. P.; Cionita, T.; Jaafar, J.; Efriyohadi, A.; Junid, R.; Kholil, A. Water Absorption Behaviour on the Mechanical Properties of Woven Hybrid Reinforced Polyester Composites. *Int. J. Adv. Manuf. Technol.* **2019**, *104*, 1075−1086.
(45) Wang, W.; Sain, M.; Cooper, P. A. Study of Moisture Absorption in Natural Fiber Plastic Composites. *Compos. Sci. Technol.* **2006**, *66*, 379−386.

https://doi.org/10.1021/acsomega.3c00353
ACS Omega 2023, 8, 20389−20403